High-temperature oxidation behavior of SiBN fibers in air

Xin Long (longxin10@nudt.edu.cn)
National University of Defense Technology College of Aerospace Science and Engineering
https://orcid.org/0000-0002-6284-9339
Zhenyu Wu
National University of Defense Technology College of Aerospace Science and Engineering
Changwei Shao
National University of Defense Technology College of Aerospace Science and Engineering
Xiaozhou Wang
National University of Defense Technology College of Aerospace Science and Engineering
Yingde Wang
National University of Defense Technology College of Aerospace Science and Engineering

Research Article

Keywords: microwave-transparent, SiBN fiber, high temperature, oxidation resistance

Posted Date: December 10th, 2020

DOI: https://doi.org/10.21203/rs.3.rs-123799/v1

Abstract

SiBN fibers are one of the most admirable microwave-transparent reinforced materials for high Mach number aircrafts. Currently, the detailed high-temperature oxidation behavior of SiBN fibers have not been studied yet. In this work, we researched the high-temperature oxidation behavior of SiBN fibers with different boron contents at the temperature range of 1000 ~ 1400℃ in air. SiBN fibers started to be oxidized at 1100℃, with Si_3N_4 and BN phase oxidized to SiO_2 and B_2O_3, respectively. Due to the gasification and the escape of molten B_2O_3 at high temperature, amorphous SiO_2 could be remained at the fiber surface. As the fiber further oxidized, the molten B_2O_3 at the inside may infiltrate into the fiber interior to react with Si_3N_4, causing the precipitation of *h*-BN nanoparticles and the formation of SiO_2/BN layer. Finally, complex oxidation layers with two distinct concentric sublayers accompanied with two transition sublayers could be formed after the oxidizing treatment.

1. Introduction

With the flight speed of aircrafts increased to a higher Mach number, the aerodynamic heating effect could be more drastic, which caused huge challenge to the thermal protection of the components in hot end, especially for the radomes that used as the communication windows [1, 2]. High temperature microwave-transparent composites (MTCs) are one of the most admirable material system to prepare radomes due to their high mechanical strength, low dielectric constant, high-temperature stability, excellent oxidation resistance, *et al* [3 ~ 5]. The reinforced fiber materials are the mainly component of the MTCs, consequently, present the great bear on the high-temperature and microwave-transparent properties of the MTCs.

At present, the developed reinforced fibers for preparing MTCs are quartz fibers [6], mullite fibers [7], Si_3N_4 fibers [8], BN fibers [9] and SiBN fibers [10]. Among them, the application temperature of quartz fibers, mullite fibers and Si_3N_4 fibers was 900℃, 1200℃ and 1300℃, respectively. BN fibers could be stable at temperature higher than 1900℃, while showed poor oxidation resistance. SiBN fibers combining the outstanding oxidation resistance of Si_3N_4 fibers and the excellent thermal stability of BN fibers, are the most promising wave-transparent reinforcement among these fibers [10, 11].

However, the preparation of high-quality SiBN fibers is still a huge challenge due to the complex fabrication process and high sensitive of precursor [12, 13]. Thus, almsost all of the researches focused on optimizing the fabrication process, while the researches related to the high-temperature properties of SiBN fibers are still lacking, especially for their oxidation resistance at high temperature, which is very important for their actual applications in reinforcing the MTCs that used in high-temperature oxidation atomsphere. To our knowledge, the detailed investigation on the oxidation behavior of SiBN fibers have not been studied yet. Nowadays, only the oxidation behavior of similar ceramic fibers such as Si_3N_4 fibers and SiBCN fibers have been investigated in detial. For example, Li and *et al* found Si_3N_4 fibers formed complex sublayers after oxidizing in air [14]. Cinibulk and coworkers investigated the oxidation behavior

of SiBCN fibers [15]. They also observed the complex sublayers with three distinct concentric layers, each increasing in oxygen concentration from the core to the outer surface. The fibers suffered significant strength degradation after the oxidation treatment. SiBN fibers showed different chemical composition from Si_3N_4 fibers and SiBCN fibers, thus, should present different oxidation behavior and oxidation layer microstructures.

In recently, large-scale continuous SiBN fibers were prepared according to our previous works [16]. The obtained SiBN fibers showed excellent high-temperature stability up to 1600℃ in inert atmosphere. In this work, these SiBN fibers with different boron contents were treated at the temperature range of 1000 ~ 1400℃ in air. The oxidation behavior as well as the microstructural evolution and mechanical properties of the SiBN fibers at high temperature have been discussed through the whole paper.

2. Experimental Section

2.1. Materials

SiBN fibers were prepared according to our previous works [16 ~ 18]. Four kinds of SiBN fibers were named as SNB-0, SNB-3, SNB-5 and SNB-7 fibers according to their boron contents. The chemical composition and the mechanism properties are listed in Table 1.

Table 1
Basic parameters for the chemical and physical properties of SiBN fibers.

Fibers	Chemical composition (wt%)					Strength (GPa)	Modulus (GPa)	Diameter (μm)
	Si	B	N	C	O			
SNB-0	60.4	0.23	36.7	0.77	2.15	1.38 ± 0.25	137 ± 5	12.8 ± 0.6
SNB-3	58.3	3.56	35.4	0.46	2.33	1.09 ± 0.21	110 ± 7	12.9 ± 0.9
SNB-5	56.1	5.14	35.8	0.58	1.60	1.47 ± 0.22	135 ± 5	12.8 ± 0.7
SNB-7	56.2	6.81	34.7	0.51	1.74	1.41 ± 0.28	123 ± 6	13.4 ± 0.7

2.2. High-temperature treatments of SiBN fibers in air

For evaluating the high-temperature oxidation resistance of SiBN fibers with different boron contents in air, a 15 cm length fiber bundle supported by the firebricks was putted into a muffle furnace. The fibers were then heated with the heating rate of 5℃/min and treated at the target temperatures for 1 hour. After the oxidation treatment, all of the SiBN fibers were furnace cooled down to room temperature.

2.3. Characterization

The carbon content of SiBN fibers was determined by a Horiba carbon/sulfur analyzer EMIA-320V (Horiba, Japan). The oxygen and nitrogen content was measured by a Horiba oxygen/nitrogen analyzer EMIA-820 (Horiba, Japan). The boron content was analyzed by converting the boron into boric acid via

solving the samples into molten NaOH, and finally titrating with standard base solution. The content of silicon in the samples was calculated by the subtraction method in the percentage weight. X-ray photoelectron spectroscopy (XPS) spectra were obtained by using an Escalab 250Xi electron spectrometer (Thermo Scientific, USA) with Al Kα radiation. X-ray diffraction (XRD) studies were carried out with a Bruker AXS D8 Advance diffractometer (Bruker, Germany) with Cu Kα radiation (k = 1.54178 A°). The specimens were continuously scanned from 10° to 80° at a speed of 0.0167 °/s. Secondary ion mass spectrometry (SIMS) was analyzed by TOF.SIMS 5-100 using the Bi^+ ion with energy of 30 keV as the primary ion beam and Cs^+ ion with energy of 2 keV as the sputtering ion beam (the sputtering rate was 0.244 nm/s that related to SiO_2). Atomic force microscope (AFM) images were obtained in non-contact mode using the Dimension Fastscan system. The morphology of the samples was examined with a scanning electron microscope (SEM; HITACHI S-4800, Japan). High resolution TEM (HR-TEM) images were taken using Titan G2 60–300 with image corrector. The tensile strength of the 25 mm-long fibers was measured at room temperature using a universal strength machine (Testometric Micro 350, UK) with a load cell of 5 N and a crosshead speed of 5 mm/min. Each tensile strength data point was the average of 24 monofilaments.

3. Results And Discussion

3.1. Characters of SiBN fibers with different boron contents

Figure 1 showed the SEM micrographs of SiBN fibers with different boron contents. It can be seen that all of the fibers showed rather smooth surface and dense cross sections, no obvious defects were detected. However, the rough surface in nanoscale could be distinguished from the 3-dimensional AFM images especially for SNB-0 and SNB-3 fibers, with surface roughness (Ra) of 3.84 nm and 4.78 nm, respectively. While SNB-5 and SNB-7 fibers showed a rather lower surface roughness (Ra) of 3.25 nm and 1.85 nm, respectively. According to the tensile strength values in Table 1, it can be conclude that SiBN fibers with lower surface roughness present higher tensile strength values.

The microstructure of the obtained SiBN fibers was studied by XRD patterns, as presented in Fig. 2a. The results showed that all of the fibers were totally amorphous, without diffraction peaks detected. The TEM micrographs and the corresponding SAED patterns of SNB-5 fibers also presented the amorphous characteristic of SiBN fibers (Fig. 2b). These experimental data agreed with the results that reported from other research groups [12, 19].

For studying the chemical state of SiBN fibers, the fiber surface was analyzed by XPS, as presented in Fig. 3. The XPS spectra showed that the SiBN fibers were mainly consisted of Si, B, N as well as small amounts of C and O, which agreed well with the chemical composition analysis in Table 1. For different SiBN fibers, the intensity for the signals of B could be obviously distinguished, indicating the different boron contents for the fibers. The XPS spectra peaks of SNB-5 fibers were further analyzed by curve-fitting with Gauss-Lorentz Equation, as shown in Fig. 3b ~ d. The Si2p peak could be fitted into two peaks: the strong peak located at 101.8 eV was contributed to the Si − N bond in Si_3N_4 phase [20], while the very

weak peak located at 100.0 eV was related to the C – Si – N bond in SiC_xN_y phase. The B1s peak could be fitted with only one peak that located at 190.8 eV, indicating the boron in SiBN fibers was mainly existed in the form of B – N bond in BN phase [21]. While the N1s peak could be fitted into two peaks that located at 397.4 eV and 398.3 eV, which were related to N – Si bond and N – B bond, respectively [22]. Thus, all of the results above indicated that the SiBN fibers were mainly consisted of Si_3N_4 phase and BN phase. Meanwhile, the Si – N–B networks that distributed between Si_3N_4 phase and BN phase may also form in the fibers [16].

3.2. Oxidation behavior of SiBN fibers with different boron contents

According to the previous microstructure and composition analysis, SiBN fibers were mainly consisted of amorphous Si_3N_4, BN and properly Si – N–B networks. These components could be oxidized and formed oxide such as SiO_2 and B_2O_3, which finally caused the increasing of oxygen content for SiBN fibers after the oxidizing treatment. Table 2 listed the oxygen content for SiBN fibers with different boron contents after oxidizing at the temperature range of 1000 ~ 1400℃. When the oxidation temperature was 1000℃, the oxygen content of SNB-0 and SNB-3 fibers showed almost unchanged, while SNB-5 and SNB-7 fibers presented an oxygen content increment of about 2 wt%. These results indicated that the SiBN fibers with higher boron content consequently higher BN content, were more easily to be oxidized. As the oxidizing temperature increasing to above 1200℃, the oxygen content for all of the SiBN fibers increased obviously. As for SNB-5 and SNB-7 fibers, although they were more easily to be oxidized, the increasing rate for the oxygen content when the oxidizing temperature increasing was slower than SNB-0 and SNB-3 fibers, which may be contributed to the escape of amounts of B_2O_3 at high temperatures.

Table 2
Oxygen content of SiBN fibers after oxidizing at different temperatures in air for 1 hour

Temperature (℃)	Oxygen content (wt%)			
	SNB-0	SNB-3	SNB-5	SNB-7
As received	2.15 (/)*	2.33 (/)	1.60(/)	1.74(/)
1000	2.70 (0.55)	2.15 (-0.18)	3.58 (1.98)	4.06 (2.32)
1200	3.24 (1.09)	3.88 (1.55)	4.55 (2.95)	4.83 (3.09)
1300	4.35 (2.20)	5.29 (2.96)	5.44 (3.84)	5.06 (3.32)
1400	6.62 (4.47)	6.75 (4.42)	6.56 (4.96)	6.55 (4.81)

* The numbers in the parentheses are the oxygen-content increment that comparing with the as received fibers.

For studying the microstructure evolution of SiBN fibers after oxidizing treatment, all of the fiber surface after oxidizing at 1300℃ for 1 hour was analyzed by XPS, as presented in Fig. 4. The results showed that

the all of the fiber surface was mainly consisted of Si and O, while the B was not detected, indicating the escape of boron in the form of B_2O_3 gas at high temperature, which agreed well with the chemical composition analysis. From the fitting cures for the Si2p peak of the oxidized SNB-5 fibers that located at the position of 104.0 eV, the chemical composition of the fiber surface was determined to be SiO_2, which was formed by the oxidation of Si_3N_4 phase [23].

The microtopography of SiBN fibers after the oxidizing treatment was observed by SEM. Figure 5 presented the SEM micrographs of fiber cross section and surface for SiBN fibers with different boron contents after oxidizing at 1300℃ for 1 hour. The results showed that the oxidized SNB-0 fibers presented an oxidation layer of 304 nm, with the formation of obvious cracks between the oxidation layer and fiber interior. The thickness of the oxidation layer for SNB-3 and SNB-5 fibers was 274 nm and 318 nm, which was very close to SNB-0 fibers. However, the interface between the oxidation layer and fiber interior showed rather dense, which is different from the interface of SNB-0 fibers. This phenomenon may be contributed to the self-healing effect when part of the molten B_2O_3 infiltrated into the oxidation interface. As for SNB-7 fibers, the oxidation layer was showed the lowest thickness of 217 nm, which should be caused by the excessive volatilization of B_2O_3 gas at high temperature.

Figure 6 showed the SEM micrographs of SNB-5 fibers after oxidizing at 1000 ~ 1400℃ for 1 hour. When the oxidizing temperature reached 1000℃, there was no obvious oxidation layer observed on the fiber cross section. As the oxidizing temperature increased to 1200℃, the oxidation layer with thickness of about 185 nm was detected. When the oxidizing temperature reached to 1300℃ and 1400℃, the thickness of oxidation layer could increase to 318 nm and 512 nm, respectively. The increasing of the oxidation layer thickness was corresponded with the increasing of oxygen content. From the SEM micrographs of the fiber surface, it can be seen that SNB-5 fibers remained smooth surface even after oxidizing at 1400℃, without detecting the obvious cracks that caused by the mismatch of thermal expansion between the oxidation layer and fiber interior. The smooth surface may be benefit for fibers to remain a rather high mechanical properties after the oxidizing treatment, which will analyzed in the following discussion.

For analyzing the oxidation process of SiBN fibers, the microstructure of oxidation layer was first investigated by the secondary ion mass spectroscopy (SIMS). Figure 7 showed the SIMS depth analysis results of the surface for SNB-5 fibers after oxidizing at 1300℃ for 1 hour. According to the intensity of the sputtering oxygen ion signals, the thickness of the oxidation layer for SNB-5 fibers after oxidizing was about 330 nm, which agreed very well with the thickness value that obtained from the SEM micrographs. Meanwhile, the oxidation layer was followed by a 75 nm depth region with the oxygen ion signals gradual decreasing, which indicated the formation of transitional oxidation layer between the oxidation layer and the fiber interior. By analyzing the intensity of boron ion signals, the oxidation layer could be finely divided into three refined microstructural layer: the outside layer with thickness about 150 nm showed very weak boron ion signals, thus this layer was mainly consisted of SiO_2, also indicating the escape of boron in the form of B_2O_3 gas at the fiber surface. The following layer was a transitional region with thickness of

about 50 nm, where the intensity of boron and nitrogen ion signals increased gradually as the testing depth increasing. Considering the boron content increased along with the nitrogen content, the boron atoms and nitrogen atoms may exist in the form of BN phase, which could be precipitated from the reduction between Si_3N_4 and the inspersed B_2O_3. Previous reports also found the precipitated BN in the oxidation layer of SiBCN fibers [15, 24]. With the depth analysis further increasing, the ion signals of boron, nitrogen and oxygen remained stable at the layer with thickness of about 140 nm. This layer presented rather high boron content may consist of more amount of BN could precipitate from the oxidation layer, which finally formed the SiO_2/BN layer.

The microstructure of the oxidizing layer was further studied by analyzing the FIB slice of SNB-5 fibers after oxidizing in air at 1300℃ for 1 h. From the TEM micrograph of the slice (Fig. 8a) as well as the enlarged micrograph (Fig. 8f), the oxidation layer could be clearly divided into three layers: the outside layer (Ⅰ) with about 200 nm thickness was totally amorphous SiO_2. The following layer (Ⅱ) with thickness about 150 nm showed the precipitation of nanoparticles. The HR-TEM micrographs presented that the nanoparticles was *h*-BN with interplanar spacing of 0.34 nm. Thus, these results showed the direct evidence for the existence of SiO_2/BN layer. Meanwhile, there is a thin interfacial layer (Ⅱ′) with thickness of about 60 nm, which distributing between the SiO_2/BN layer and the fiber interior was the transition region. The formation of three layers in the oxidation layer agreed well with the SIMS results in Fig. 7 (The transition layer between SiO_2 and SiO_2/BN layer was unobvious to be detected in the TEM micrographs).

According to the SIMS and TEM analysis, the microstructure for the oxidation layer of SiBN fibers could be described by the model in Fig. 9a, in which the oxidation layer could be divided into SiO_2 layer and SiO_2/BN layer. Meanwhile, two different transition layer could also be observed, one was distributed between the SiO_2 layer and SiO_2/BN layer, the other was formed between the SiO_2/BN layer and unoxidized fiber interior. Based on the microstructural model of the oxidation layer, the oxidizing process of SiBN fibers could be described as the schematic diagram in Fig. 9b. When SiBN fibers were oxidized in the air at high temperature, the BN and Si_3N_4 phase in fibers could be oxidized to form the oxide such as B_2O_3 and SiO_2, respectively (Reaction 1 and 3). In the fiber surface, the molten B_2O_3 was easily to escape as gas state at high temperature (Reaction 2). Thus, the fiber surface after oxidizing was mainly consisted of remained SiO_2. As the fiber further oxidized, the molten B_2O_3 formed at the inside may infiltrate into the fiber interior to react with Si_3N_4, which finally caused the precipitation of *h*-BN nanoparticles (Reaction 4), as consequently, formed the SiO_2/BN layer. All of the layer with different chemical compositions presented the formation of transition layer due to the diffusion-controlled oxidizing process. The infiltration of molten B_2O_3 may act as the self-healing composition, which is benefit for reducing the cracks in the fibers.

$2BN(s) + 1.5O_2(g) = B_2O_3(l) + N_2(g)$	**(Reaction 1)**
$B_2O_3(l) = B_2O_3(g)$	(Reaction 2)
$Si_3N_4(s) + 3O_2(g) = 3SiO_2(s) + 2N_2(g)$	(Reaction 3)
$2B_2O_3(l) + Si_3N_4(s) = 3SiO_2(s) + 4BN(s)$	(Reaction 4)

Figure 10 calculated the changes of the standard Gibbs free energy of Reaction 1 ~ 4 in the temperature range of 1000 ~ 2000℃. The results showed that the standard Gibbs free energy of Reaction 1, 3 and 4 was negative, indicating these reactions could occur at above 1000℃. As for Reaction 2 that related to the gasification of molten B_2O_3, the standard Gibbs free energy was positive. However, when considering the very low partial pressure of B_2O_3 in the air, the Reaction 2 could occur to balance the equilibrium of reaction. Thus, the calculated results confirmed the reactions that mentioned in the oxidation process (Fig. 9b).

3.3. The tensile strength of SiBN fibers after the oxidation tests

The tensile strength of SiBN fibers after the oxidation treatment is one of leading indicator to evaluate their high-temperature oxidation resistance. Figure 11 presented the tensile strength and the strength retention of SiBN fibers with different boron contents after oxidizing at 1300℃ in air for 1 hour. As for SNB-0 fibers, the remained tensile strength and strength retention was 0.6GPa and 44%, respectively, while SNB-3, SNB-5 and SNB-7 fibers showed a rather higher tensile strength (~ 0.7GPa) and strength retention (> 50%) after the oxidizing treatment. Thus, although SiBN fibers that consisted of BN phase were easy to be oxidized, they showed enhanced oxidation resistance at high temperature, which may contribute to the self-healing effects of molten B_2O_3.

4. Conclusions

In this work, the oxidation behavior of SiBN fibers with different boron contents were studied after the treatment at the temperature range of 1000 ~ 1400℃ in air. SiBN fibers were mainly consisted of Si_3N_4 and BN phase. After treating at above 1100℃, the Si_3N_4 and BN phase in SiBN fibers started to be oxidized, with the formation of SiO_2 and B_2O_3, respectively. Meanwhile, at the fiber surface, the molten B_2O_3 was easily to escape as gas state at high temperature, causing the remaining of SiO_2 layer. As the fiber further oxidized, the molten B_2O_3 at the inside may infiltrate into the fiber interior to react with Si_3N_4, causing the precipitation of *h*-BN nanoparticles and the formation of SiO_2/BN layer. Finally, complex oxidation layers with two distinct concentric sublayers accompanied with two transition sublayers could be formed after the oxidizing treatment in air. The infiltration of molten B_2O_3 may act as the self-healing composition, which is benefit for reducing the cracks in the fibers.

Declarations

Conflict of interest

There are no conflicts of interest to declare.

Acknowledgments

This work is supported by the National Natural Science Foundation of China (52073304).

References

1. Padture NP. Advanced structural ceramics in aerospace propulsion. *Nat Mater* 2016, **15**: 804–809.
2. Khatavakar N, Balasubramanian K. Composite materials for supersonic aircraft radomes with ameliorated radio frequency transmission-a review. *RSC Adv* 2016, **6**: 6709–6718.
3. Zou CR, Li B, Wang SQ, et al. Fabrication and high-temperature mechanical properties of 2.5DSi_3N_{4f}/BN fiber-reinforced ceramic matrix composite. *Mater Des* 2016, **92**: 335–344.
4. Cheng ZL, Ye F, Liu YS, et al. Mechanical and dielectric properties of porous and wave-transparent Si_3N_4-Si_3N_4 composite ceramics fabricated by 3D printing combined with chemical vapor infiltration. *J Adv Ceram* 2019, **8**: 399-407.
5. Li B, Liu K, Zhang CR, et al. Fabrication and properties of borazine derived boron nitride bonded porous silicon aluminum oxynitride wave-transparent composite. *J Eur Ceram Soc* 2014, **34**: 3591–3595.
6. Zhao Z, Zhou GX, Yang ZH, et al. Direct ink writing of continuous SiO_2 fiber reinforced wave-transparent ceramics. *J Adv Ceram* 2020, **9**: 403–412.
7. Peters PWM, Daniels B, Clemens F, et al. Mechanical characterization of mullite-based ceramic matrix composites at test temperature up to 1200℃. *J Eur Ceram Soc* 2000, **20**: 531–535.
8. Ma X, Liang YY, Qiu HP. Preparation of high-performance 2D Si_3N_{4f}/SiBN ceramic matrix composites by precursor infiltration pyrolysis. IOP Conference Series: Materials Science and Engineering. IOP Publishing, 2019, 678: 012044.
9. Toury B, Miele P, Cornu D, et al. Boron nitride fibers prepared from symmetric and asymmetric alkylaminoborazines. *Adv Funct Mater* 2002, **12**: 228–234.
10. Tang Y, Wang J, Li XD, et al. Polymer-derived SiBN fiber for high-temperature structural/functional applications. *Chem Eur J* 2010, **16**: 6458–6462.
11. Li D, Zhang C, Li B, et al. Mechanical properties of unidirection SiBN fiber reinforced boron nitride matrix composites. *Mater Lett* 2012, **68**: 222–224.

12. Peng YQ, Han KQ, Zhao X, et al. Large-scale preparation of SiBN ceramic fibres from a single source precursor. *Ceram Int* 2014, **40**: 4797–4804.
13. Baldus HP, Jansen M. Novel high-performance ceramics–amorphous inorganic networks from molecular precursors. *Angew Chem Int Ed Engl* 1997, **36**: 328–343.
14. Li SW, Li Y, Xiao H, et al. Oxidation behavior of Si_3N_4 fibers derived from polycarbosilane. *Corros Sci* 2018, **136**: 9–17.
15. Cinibulk MK, Parthasarathy TA. Characterization of oxidized polymer-derived SiBCN fibers. *J Am Ceram Soc* 2001, **84**: 2197–2202.
16. Long X, Shao CW, Wang YD. Effects of boron content on the microwave-transparent property and high-temperature stability of continuous SiBN fibers. *J Am Ceram Soc* 2020, **103**: 4436–4444.
17. Ji XY, Shao CW, Wang H, et al. A simple and efficient method for the synthesis of SiBNC ceramics with different Si/B atomic ratios. *Ceram Int* 2017, **43**: 7469–7479.
18. Lu L, Feng CX, Song YC. Curing polysilazanes fibres by exposure to boron trichloride. *J Mater Sci Lett* 1998, **17**: 481–484.
19. Liu Y, Peng S, Cui YJ, et al. Fabrication and properties of precursor-derived SiBN ternary ceramic fibers. *Mater Des* 2017, **128**: 150–156.
20. Hou YB, Li B, Shao CW, et al. Effect of high-temperature annealing in air and N_2 atmosphere on the mechanical properties of Si_3N_4*Mater Sci Eng A*, 2018, **724**: 502–508.
21. Kong J, Wang MJ, Zou JH, et al. Soluble and meltable hyperbranched polyborosilazanes toward high-temperature stable SiBCN ceramics. *ACS Appl Mater Interfaces* 2015, **7**: 6733–6744.
22. Liu YS, Chai N, Li Z, et al. Effect of decomposition temperature on deposition kinetics and mechanism of silicon boron nitride coating deposited from $SiCl_4$-BCl_3-NH_3-H_2-Ar mixture using low pressure chemical vapor deposition. *Surf Coat Technol* 2015, **261**: 295–303.
23. Li DX, Yang ZH, Jia DC, et al. High-temperature oxidation behavior of dense SiBCN monoliths: carbon-content dependent oxidation structure, kinetics and mechanisms. *Corros Sci* 2017, **124**: 103–120.
24. Ji XY, Wang SS, Shao CW, et al. High-temperature corrosion behavior of SiBCN fibers for aerospace applications. *ACS Appl Mater Interfaces* 2018, **10**: 19712–19720.

Figures

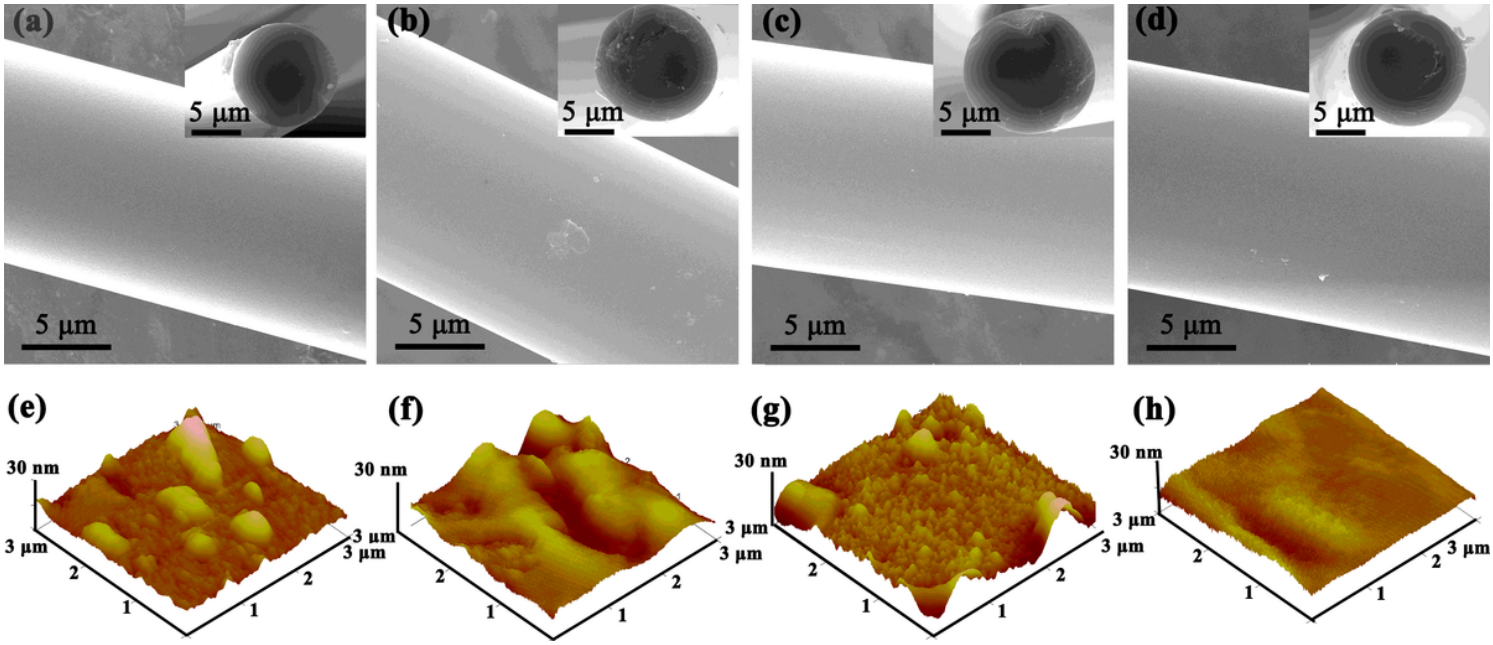

Figure 1

SEM micrographs (a, b, c and d) and AFM images of the surface morphologies (e, f, g and h) for the SiBN fibers with different boron contents: SNB-0 (a, e); SNB-3 (b, f); SNB-5 (c, g); SNB-7 (d, h).

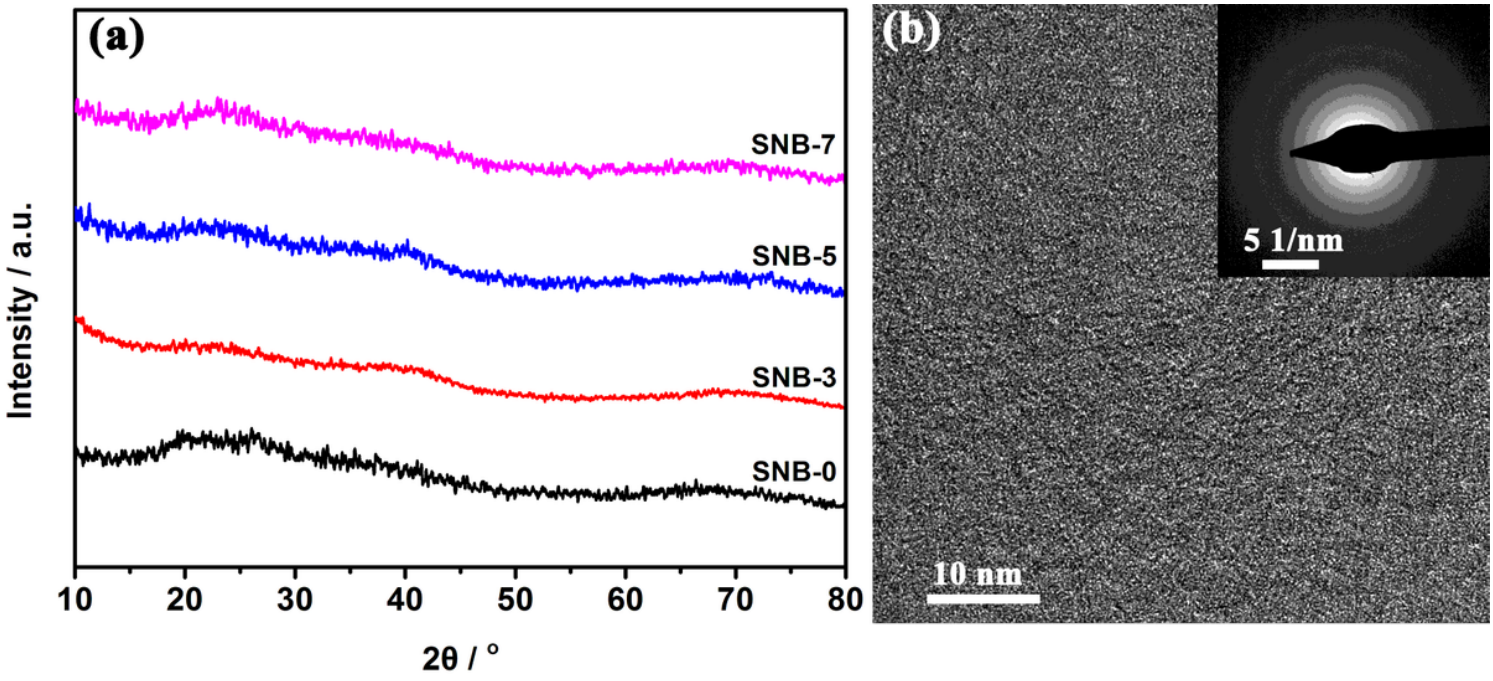

Figure 2

XRD patterns of SiBN fibers with different boron contents (a); TEM micrograph and corresponding SAED pattern of SNB-5 fibers (b).

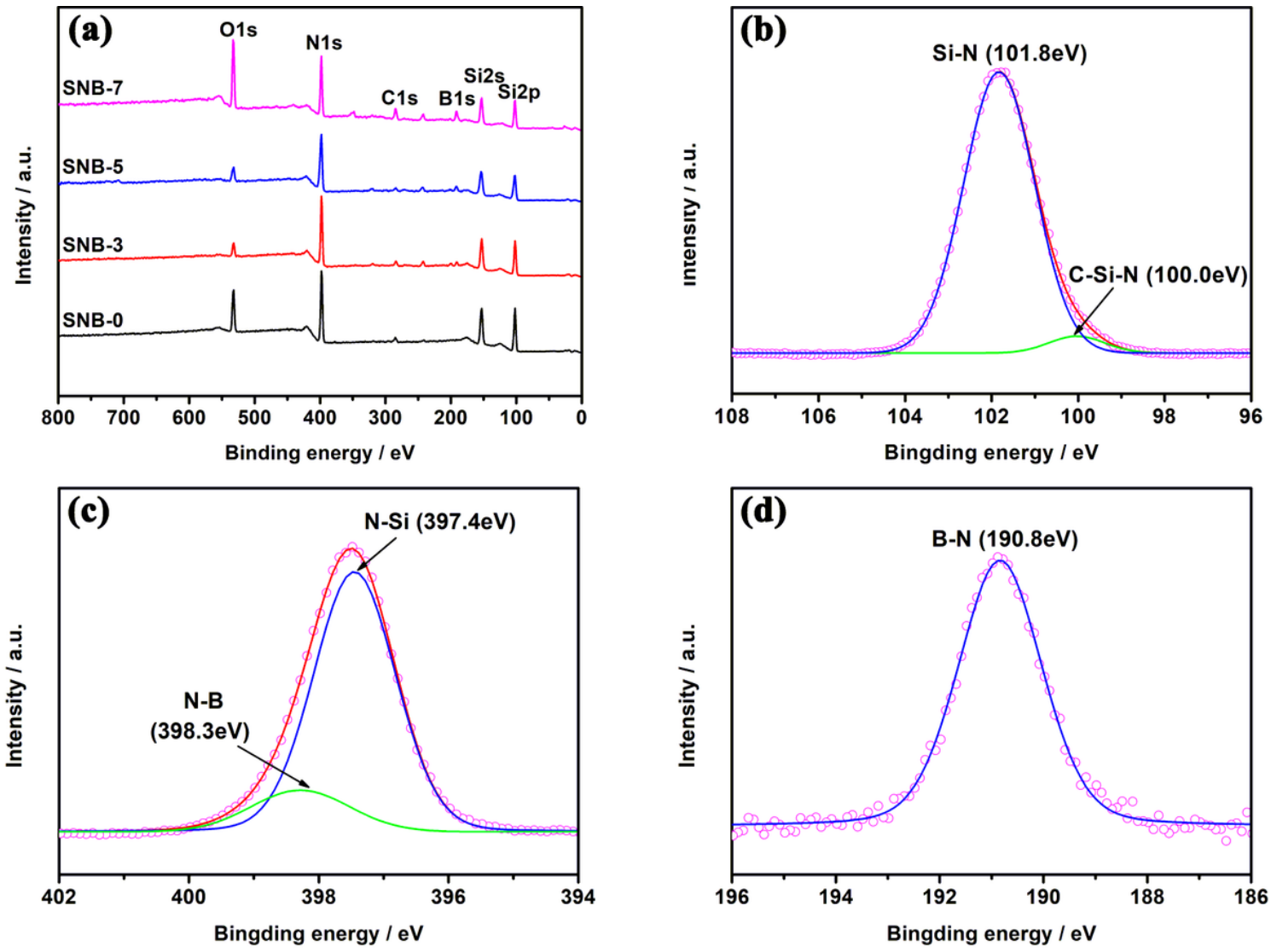

Figure 3

XPS spectra of SiBN fibers with different boron contents (a); Si2p (b), B1s (c) and N1s (d) spectra of SNB-5 fibers

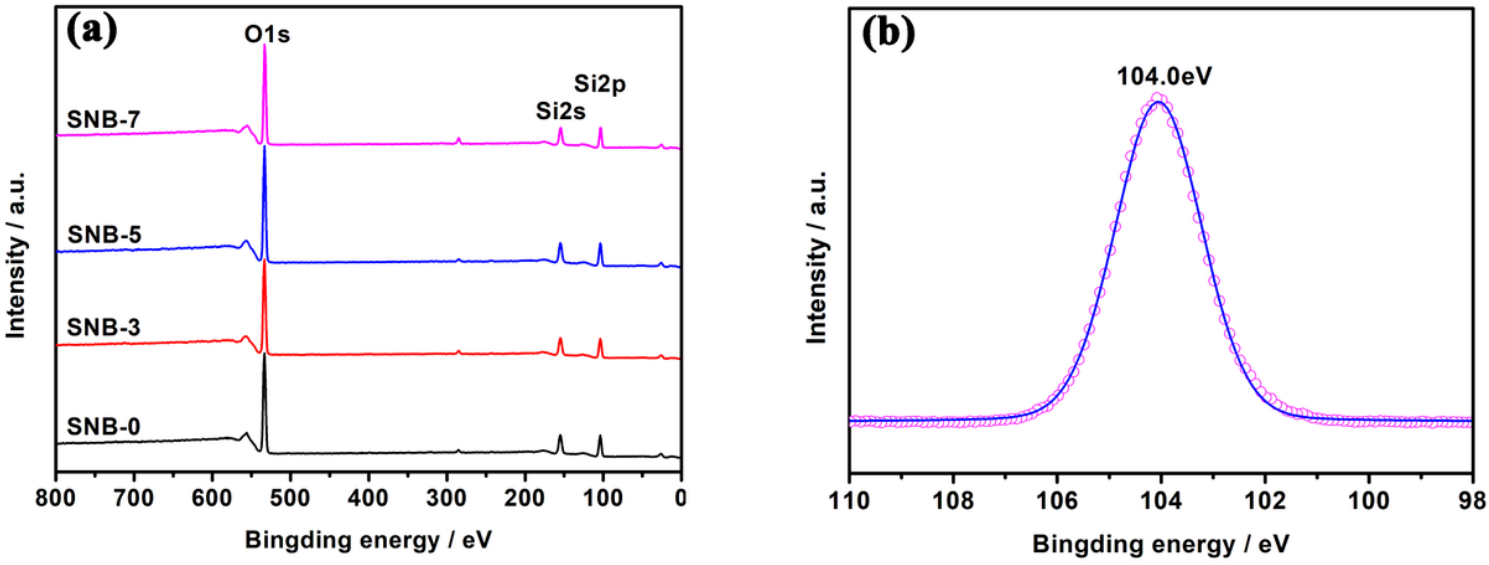

Figure 4

XPS spectra of SiBN fibers after oxidizing at 1300 ℃ in air for 1 hour (a); XPS spectra of Si2p for the oxidized SNB-5 (b)

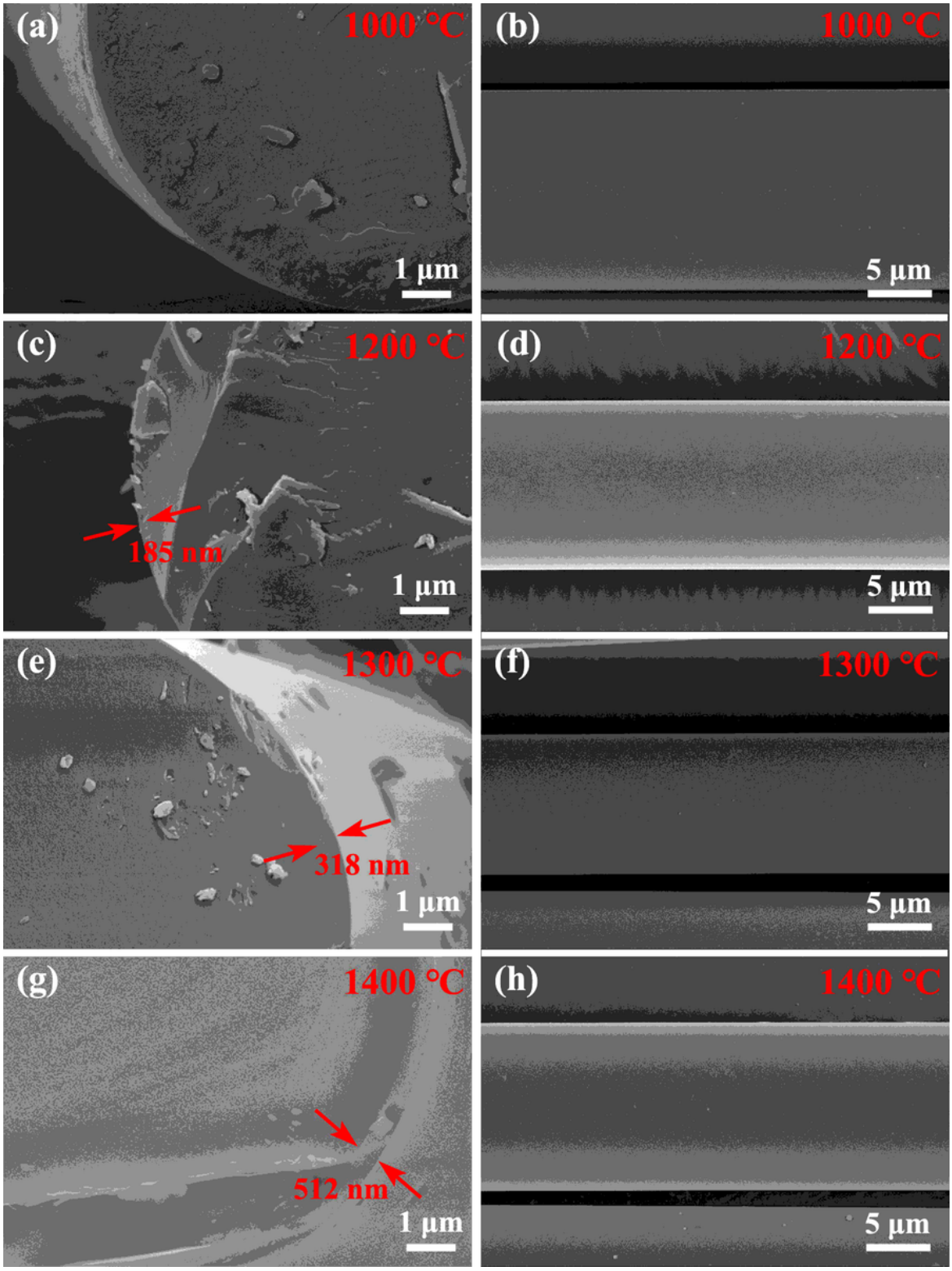

Figure 5

SEM micrographs for the fiber cross-section (a, c, e and g) and surface (b, d, f, h) of SNB-0 (a, b), SNB-3 (c, d), SNB-5 (e, f) and SNB-7 (g, h) fibers after oxidizing at 1300°C in air for 1 hour

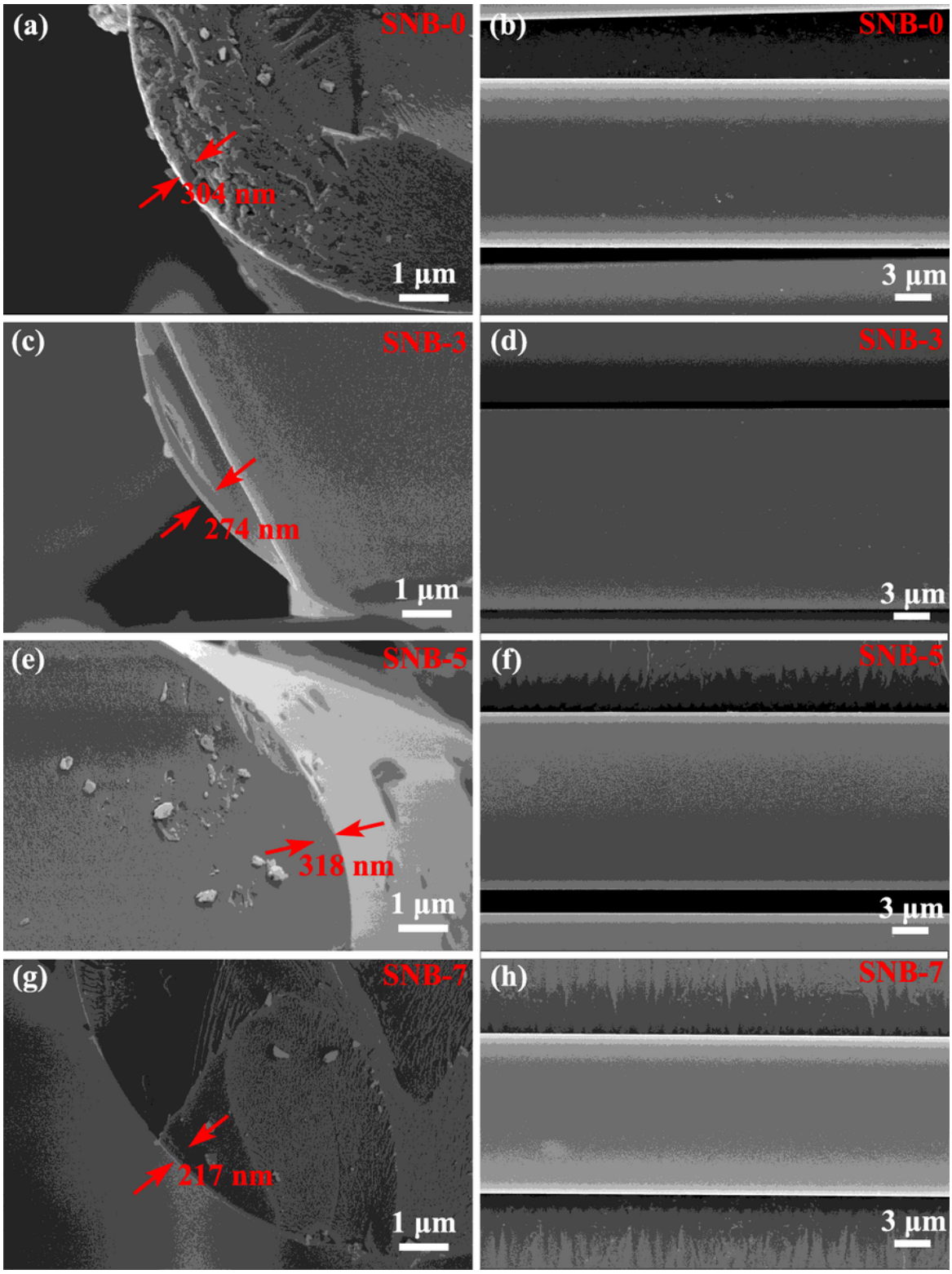

Figure 6

SEM micrographs for the fiber cross-section (a, c, e, g) and surface (b, d, f, h) of SNB-5 fibers after oxidizing at 1000°C (a, b), 1200°C (c, d), 1300°C (e, f) and 1400°C (g, h) in air for 1 hour

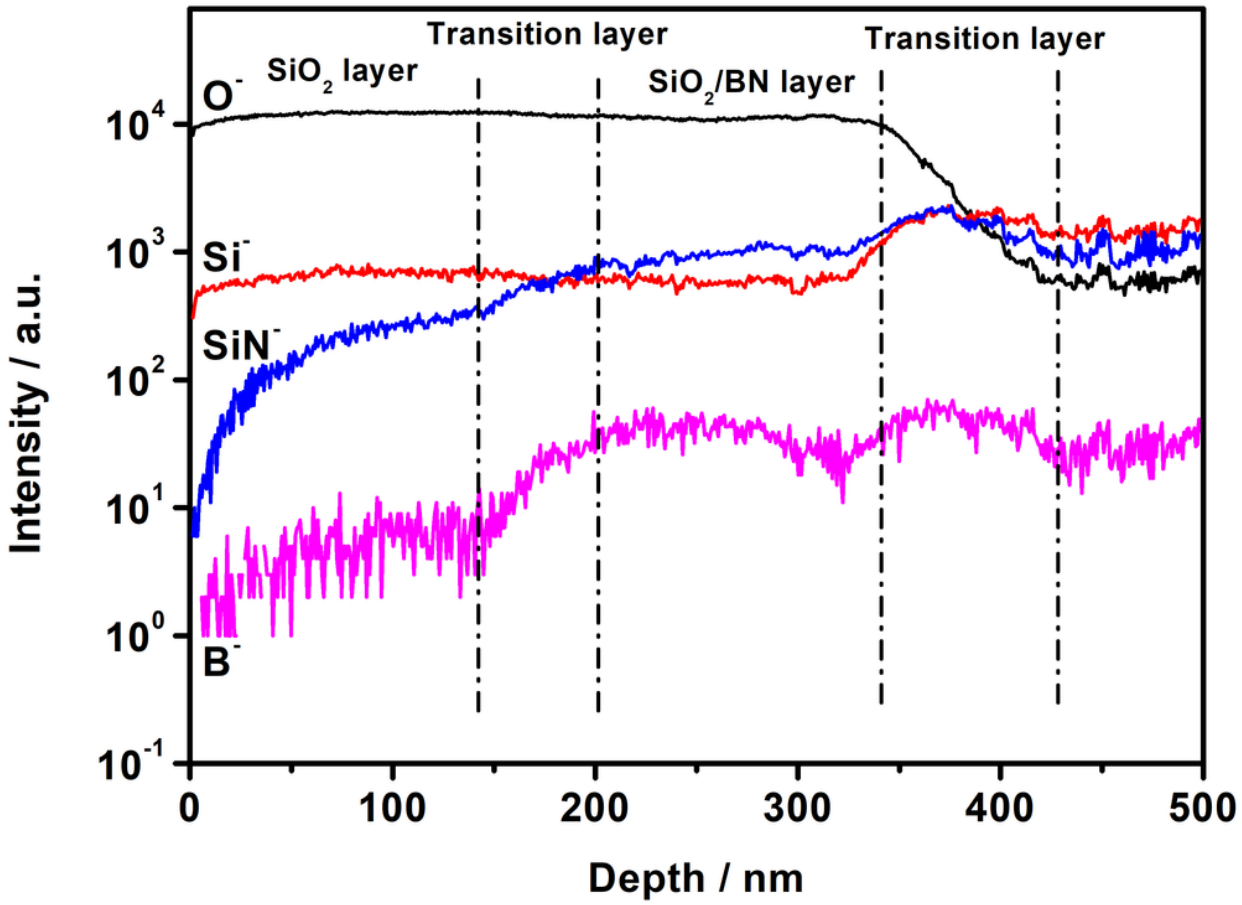

Figure 7

SIMS depth analysis of surface element content of SNB-5 fibers after oxidizing in air at 1300°C for 1 h

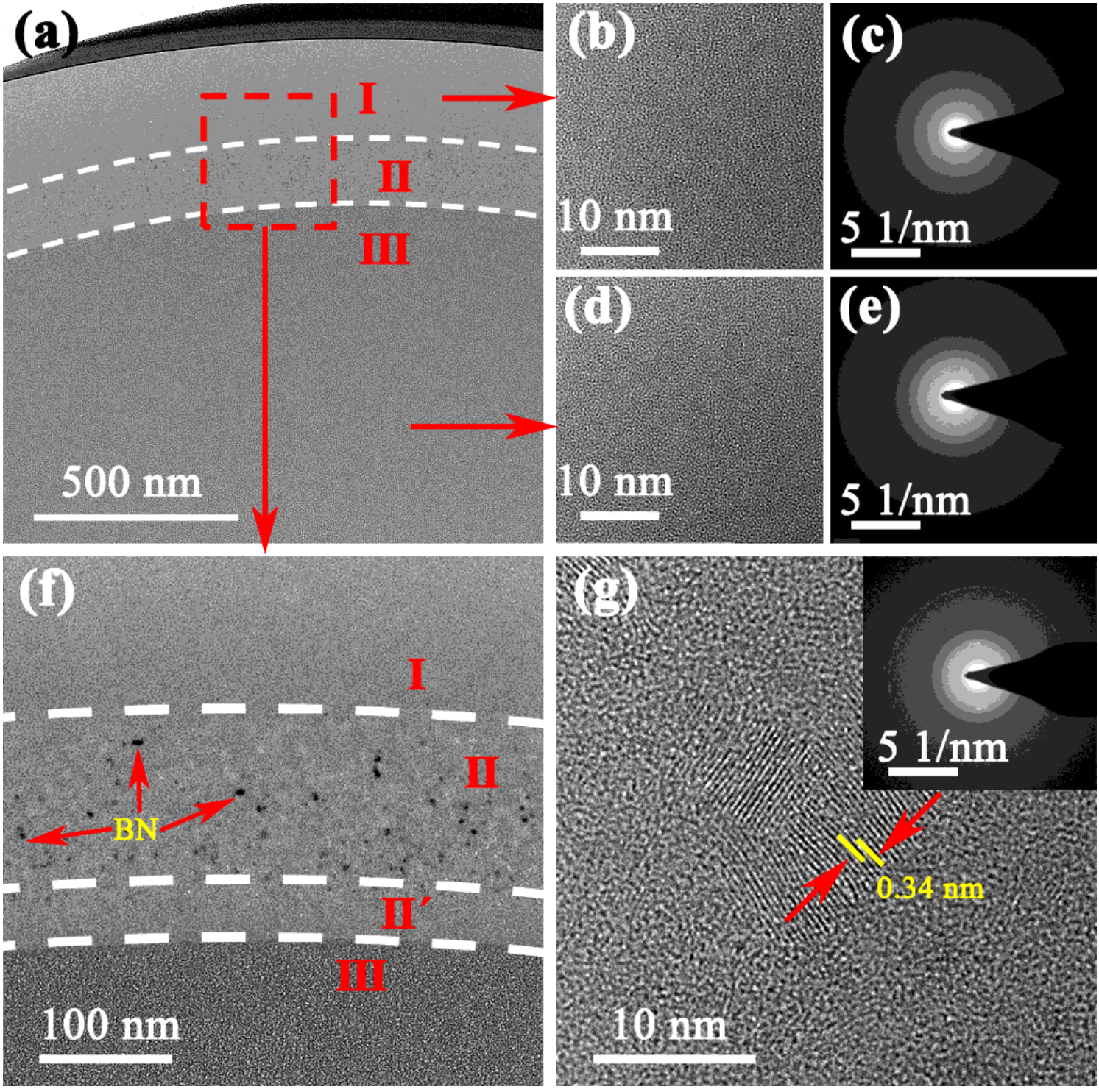

Figure 8

The TEM micrograph for the slice of SNB-5 fibers after oxidizing in air at 1300 °C for 1 h (a, f); the HR-TEM micrographs for region (b), (g), (d), as well as the corresponding SAED patterns (c: ; e:)

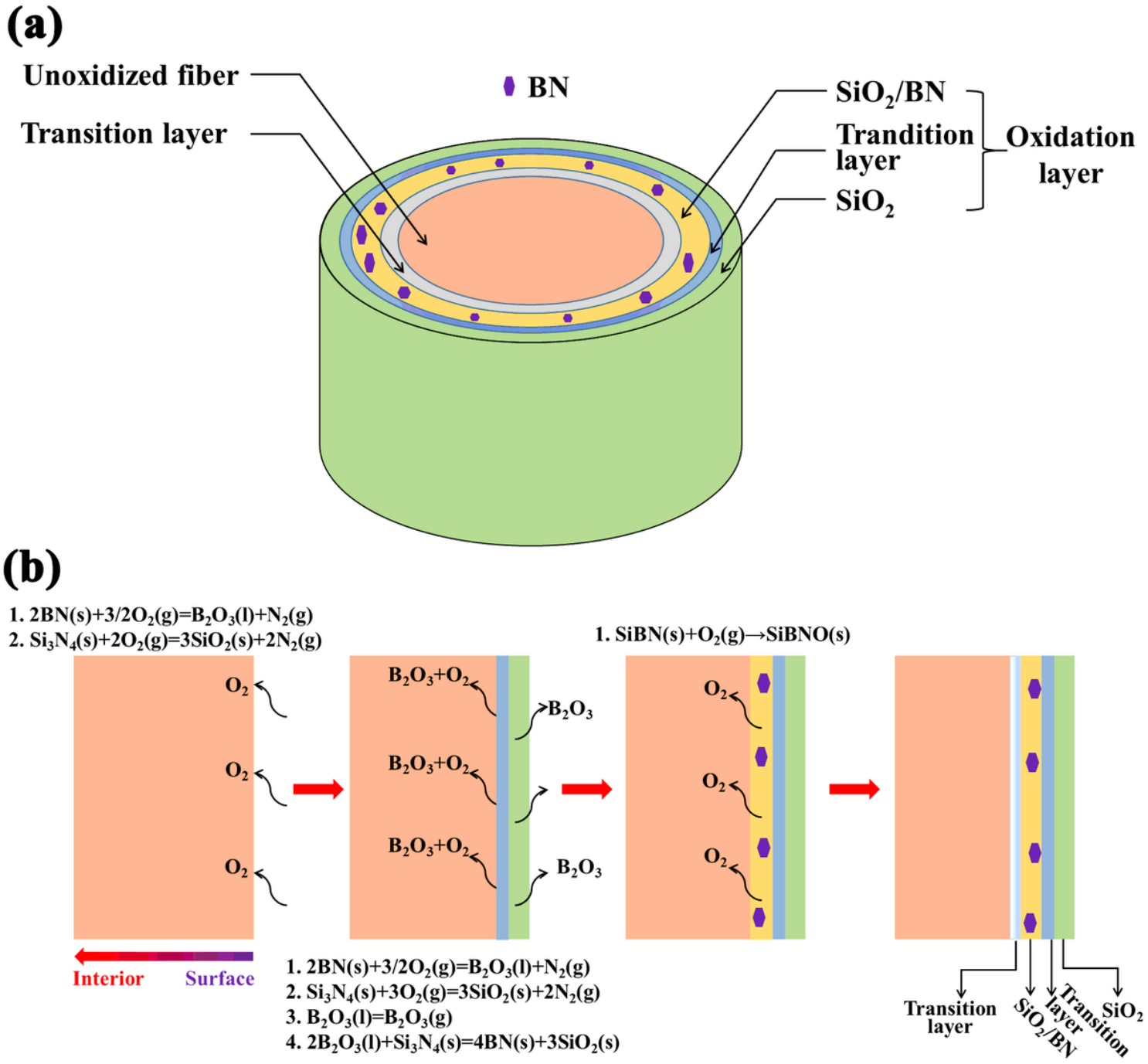

Figure 9

The microstructure model of the oxidation layer of SiBN fibers after oxidizing at in air (a); schematic diagram for the oxidation process of SiBN fibers (b)

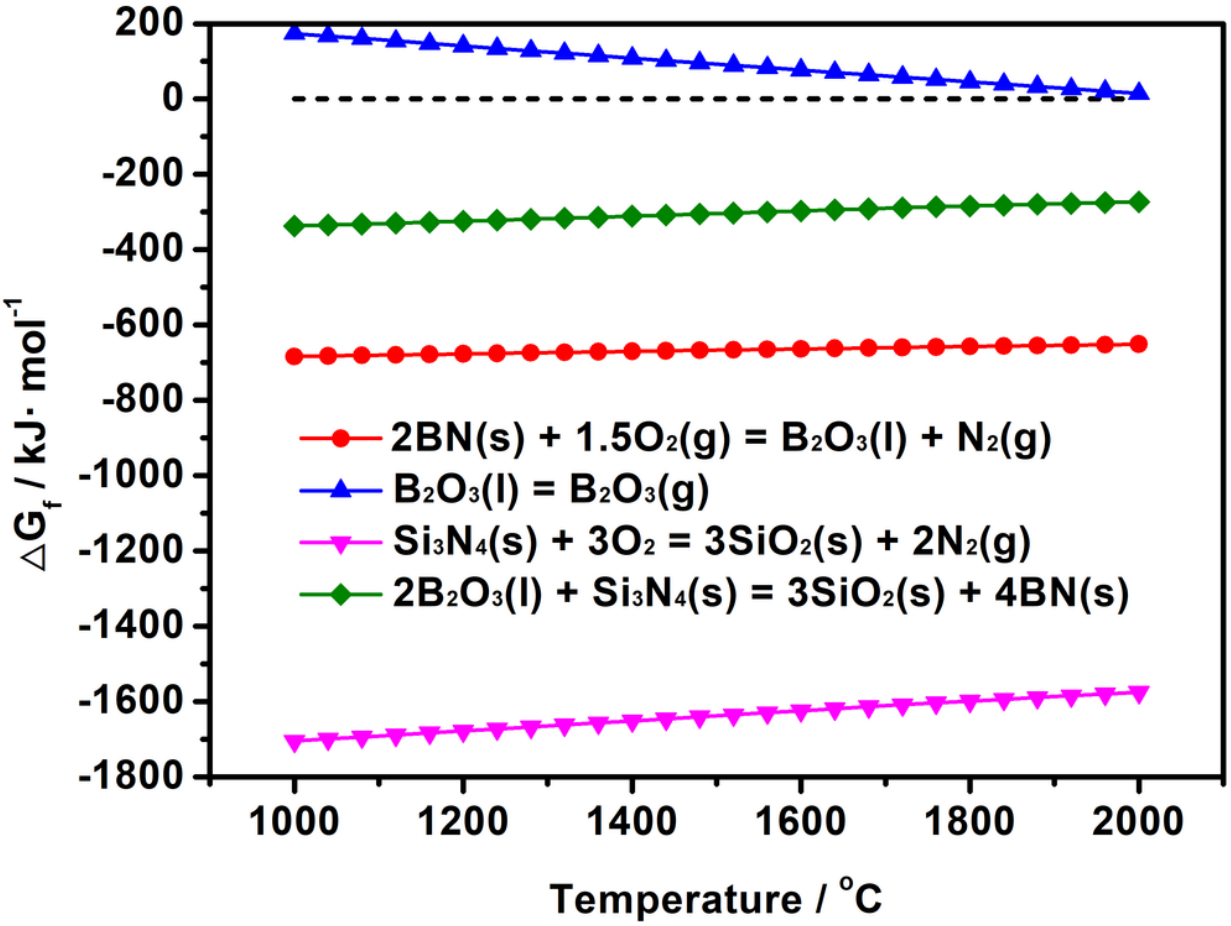

Figure 10

The calculated Gibbs free energy for the Reaction 1~4.

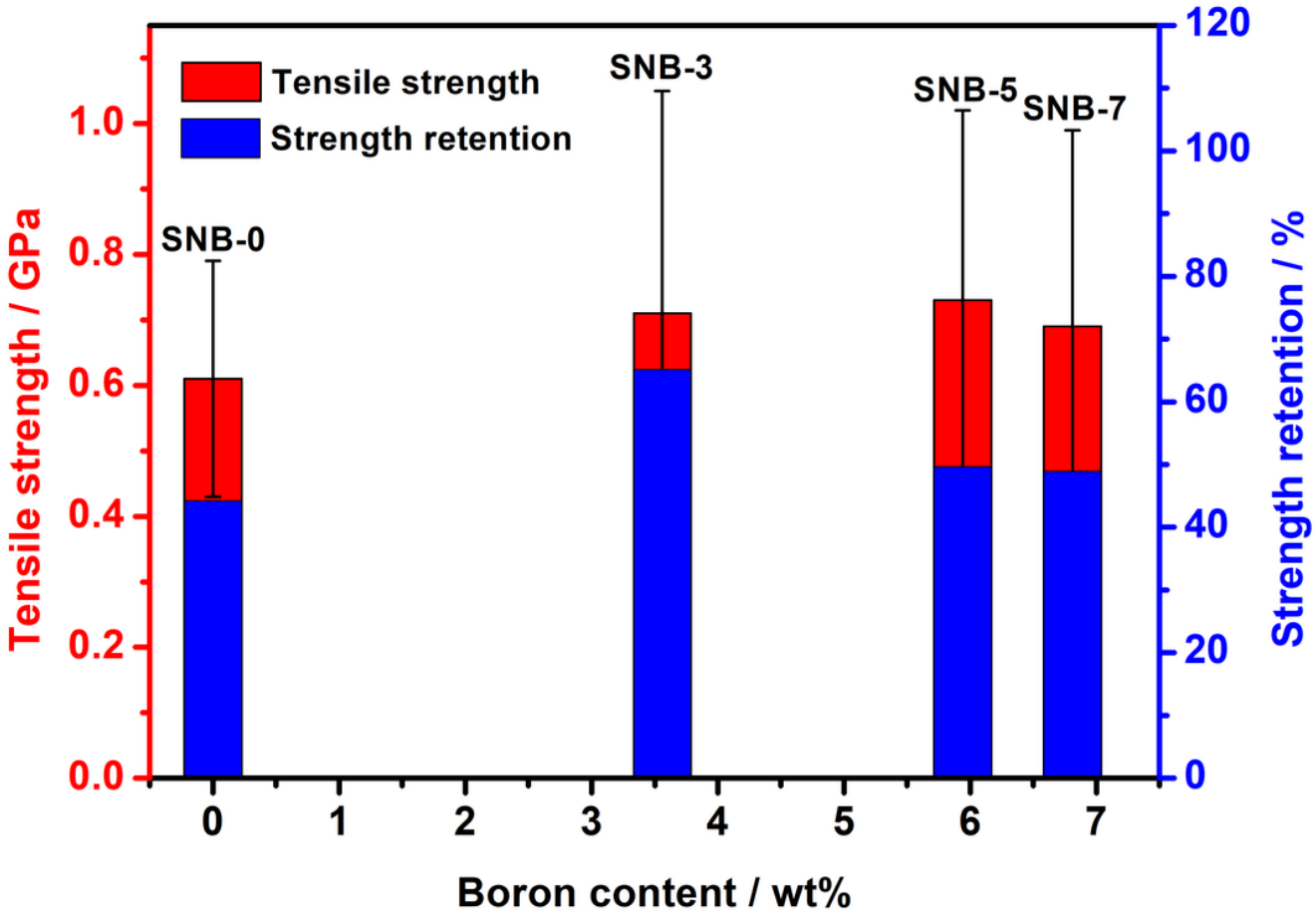

Figure 11

Tensile strength and tensile strength retention of SiBN fibers with different boron contents after oxidizing at 1300℃ in air for 1 hour